



## Modelling non-linear patterns of time-varying intervention effects on recurrent events in infectious disease prevention studies

Yin Bun Cheung, Xiangmei Ma, K. F. Lam, Chee Fu Yung & Paul Milligan

To cite this article: Yin Bun Cheung, Xiangmei Ma, K. F. Lam, Chee Fu Yung & Paul Milligan (2022): Modelling non-linear patterns of time-varying intervention effects on recurrent events in infectious disease prevention studies, Journal of Biopharmaceutical Statistics, DOI: [10.1080/10543406.2022.2108826](https://doi.org/10.1080/10543406.2022.2108826)

To link to this article: <https://doi.org/10.1080/10543406.2022.2108826>



Published online: 10 Aug 2022.



Submit your article to this journal [↗](#)



View related articles [↗](#)



View Crossmark data [↗](#)



# Modelling non-linear patterns of time-varying intervention effects on recurrent events in infectious disease prevention studies

Yin Bun Cheung <sup>a,b,c</sup>, Xiangmei Ma <sup>a</sup>, K. F. Lam <sup>a,d</sup>, Chee Fu Yung <sup>e,f,g</sup>,  
and Paul Milligan <sup>h</sup>

<sup>a</sup>Centre for Quantitative Medicine, Duke-NUS Medical School, Singapore; <sup>b</sup>Programme in Health Services & Systems Research, Duke-NUS Medical School, Singapore; <sup>c</sup>Tampere Center for Child, Adolescent and Maternal Health Research, Tampere University, Tampere, Finland; <sup>d</sup>Department of Statistics and Actuarial Science, University of Hong Kong, Hong Kong, Pok Fu Lam, China; <sup>e</sup>Infectious Disease Service, KK Women's and Children's Hospital, Singapore; <sup>f</sup>Lee Kong Chian School of Medicine, Nanyang Technological University, Singapore; <sup>g</sup>Academic Medicine Department, Duke-NUS Medical School, Singapore; <sup>h</sup>Faculty of Epidemiology and Population Health, London School of Hygiene & Tropical Medicine, London, UK

## ABSTRACT

Protective efficacy of vaccines and pharmaceutical products for prevention of infectious diseases usually vary over time. Information on the trajectory of the level of protection is valuable. We consider a parsimonious, non-linear and non-monotonic function for modelling time-varying intervention effects and compare it with several alternatives. The cumulative effects of multiple doses of intervention over time can be captured by an additive series of the function. We apply it to the Andersen–Gill model for analysis of recurrent time-to-event data. We re-analyze data from a trial of intermittent preventive treatment for malaria to illustrate and evaluate the method by simulation.

## ARTICLE HISTORY

Received 26 November 2021  
Accepted 20 July 2022

## KEYWORDS

Andersen–Gill model;  
infectious disease; non-linear  
function; protective efficacy;  
time-varying effect;  
recurrent events

## 1. Introduction

Protective efficacy of vaccines and pharmaceutical products for prevention of infectious diseases usually varies over time. There is a long-standing interest in the evaluation of the waning of protective efficacy. While some vaccines offer protection that last for years, some vaccines such as malaria and Covid-19 vaccines may have short-lived effects and booster doses are needed (Moghadas et al. 2021; RTS,S Clinical Trials Partnership 2015; Smith and Milligan 2005). Seasonal malaria chemoprevention and mass drug distribution such as preventive use of antibiotics have relatively time-limited effects and require regular re-administration (Cairns et al. 2008; Phiri et al. 2021; Porco et al. 2019). Information on the time-course of the waning effect can guide the frequency and timing of booster doses or re-administration. The pattern of initial changes in protective efficacy after dosing has received less attention. Vaccine studies typically consider 14 days after completion of the primary series as the start point of analysis time. That was the way large scale trials of, for example, pneumococcal, malaria and Covid-19 vaccines were analyzed (Cutts et al. 2005; RTS,S Clinical Trials Partnership 2015; Voysey et al. 2021). Disease risk between the first dose of vaccine and 14 days post completion of the primary series is typically not evaluated. However, the Covid-19 pandemic and global shortage of vaccines has drawn attention to the time course of the efficacy after the first dose (Moghadas et al. 2021; Skowronski and De Serres 2021). This is important with respect to the time during which a vaccinee should be assumed unprotected, and whether the second dose can be delayed such that the vaccine supply can be prioritized for distribution as the first dose to more people.

Individuals exposed to infectious diseases may acquire partial or complete immunity. A short-term success in the prevention of an infectious disease may lead to a reduced rate of acquisition of natural immunity and consequently an elevated disease risk in the long-term. This is known as (negative) event dependency in the statistics literature (Cheung et al. 2010; Xu et al. 2012) and rebound effects in the infectious disease literature (Grobusch et al. 2009; Odhiambo et al. 2010). The concern for rebound effects delayed the widespread deployment of insecticide-treated bednets (Nahlen et al. 2003). Statistical analysis that can demonstrate the likelihood of a rebound effect is useful for clinical recommendation and policy making.

Various attempts have been made to estimate “duration of protection” offered by disease prevention measures. However, the search for a duration of protection may be over-simplifying because implicitly it assumes a pattern of a sharp change from a high to a low level of efficacy. How common such a pattern is has remained largely unknown. Studying the changes of protection level over time is more informative. One approach is to partition follow-up time into intervals (Cairns et al. 2008; Cheung et al. 2020; Lopez Bernal et al. 2021; Phiri et al. 2021), assuming a step function. However, it suffers irregular fluctuations if the intervals are narrow, especially when sample size is not very large, and it loses informativeness if the intervals are wide. Some investigators resorted to comparing the densities of time from intervention or placebo to outcome event among those who did suffer the outcome event (Porco et al. 2019). This can be biased if there are different patterns of censoring between participants with different intervention status or if the intervention generates a non-susceptible fraction (Xu et al. 2012). In the studies of non-repeatable events, investigators have employed smooth, monotonic functions to capture time-varying effects (Cheung et al. 2001; Kanaan and Farrington 2002).

Many infectious diseases can recur, as opposed to diseases that offer lifetime immunity after one episode of the disease. Malaria and pneumonia are some examples of diseases of public health importance in which disease episodes can recur. In 2008, the World Health Organization Malaria Vaccine Advisory Committee called for methodology research on analysis of recurrent events (Moorthy et al. 2009). Around that time, the popular research practice was to analyse only the first disease episode even if multiple episodes were observed from the same person. This practice risks over-emphasizing short-term efficacy and makes difficult the charting of waning effects. Various models for recurrent time-to-event data have been proposed and evaluated; some are difficult to interpret (European Medicines Agency 2020; Kelly and Lim 2000; Metcalfe and Thompson 2007). The Andersen–Gill (AG) model, which is an extension of the Cox model, has been found useful in clinical research (Cheung et al. 2010; Jahn-Eimermacher et al. 2017; Rauch et al. 2018). Earlier simulation studies suggested that the AG model gave biased estimates and they did not recommend the use of this model. However, it has been shown that it was a common procedure in their simulation methods, not the AG model, that generated the bias (Cheung et al. 2010). Recent research has also highlighted that the choice of models depends on the target of estimation, i.e. the estimand (Cheung et al. 2020; Jahn-Eimermacher et al. 2017; Rauch et al. 2018). The AG model provides unbiased estimation of the total effect, also called composite effect, which includes the secondary impact of the intervention via rebound effects (event dependency). It has been proposed that the total effect is an important estimand from a public health point of view. If rebound effects are considered a nuisance, alternative models are needed. In the present context, the AG model is the model of choice since rebound effects is a real-life concern in public health.

The basic form of the AG model (and other Cox-type models) assumes time-constant intervention effects applied to the hazard function, i.e. the proportional hazard (PH) assumption. A previous study proposed a 4-parameter function that captures a monotonic, non-linear pattern of time-varying effects in the AG model (Xu et al. 2017). An advantage of this function is that the four parameters are interpretable, representing the level of short-term effect, rate of waning, shape of the waning trajectory and level of long-term effect, respectively. Furthermore, an additive series of the function can be used to model the ups and downs of the protection level over re-administration of the intervention, with each element in the series capturing the impact of the latest dose. However, this function assumes

protective efficacy to change from zero to peak level practically immediately upon dosing. Alternatively, the application of the monotonic function should be limited to analysis that begins when the peak level is supposed to have been reached. While this may work for some fast-acting products such as monoclonal antibodies and the typical vaccine trial analysis that focuses on disease incidence at least 14 days after completion of the primary series, a non-monotonic function that captures the whole trajectory from zero to peak to waning is useful for the evaluation of slower-acting products.

The aim of this study is to propose and evaluate a 4-parameter non-monotonic, non-linear function of time-varying effects for the AG model for recurrent events, and to compare it with the 4-parameter monotonic function and more flexible but less interpretable or less parsimonious models using splines and step functions.

## 2. Statistical models

### 2.1. Andersen–Gill model with time-varying effects and repeated dosing

Let  $N$  be the number of subjects who belong to either an intervention group or a control group. Define  $z_i$  to be an indicator variable with  $z_i = 1$  if the  $i$ -th subject is in the intervention group and  $z_i = 0$  otherwise. Let  $0 < t_{i1} < t_{i2} < \dots < t_{i,n_i}$  be the recurrent event times,  $n_i$  be the number of events the  $i$ -th subject experiences, and  $\tau_i$  be the subject’s total follow-up time or censoring time. The AG model for time-varying effect models the hazard of the outcome event for subject  $i$  at time  $t$  as:

$$\lambda_i(t) = \lambda_0(t) \exp[\boldsymbol{\gamma}^T \boldsymbol{x}_i(t) + z_i G(t)] \tag{1}$$

where  $\lambda_0(t) \geq 0$  is an unspecified baseline hazard function,  $\boldsymbol{x}_i(t)$  is a vector of possibly time-varying covariates,  $\boldsymbol{\gamma}$  is the vector of coefficients for  $\boldsymbol{x}_i(t)$ , and  $G(t)$  is the function of the time-varying effect of the intervention that is the key interest (Xu et al. 2017). In infectious disease research, protective efficacy (PE) equals  $1 - \text{hazard ratio (HR)}$ . In the present context,

$$PE(t) = 1 - \exp[G(t)].$$

For an intervention regime that involves up to  $m$  doses, define  $0 \leq d_{i1} < d_{i2} < \dots < d_{im}$  be the times at dosing, which in practice are variable across subjects because of non-compliance or other real-life issues. Due to such variation, allowing the effect of  $z_i$  to vary over time would not properly describe the effect of the doses of the intervention. To allow for the variation,  $G(t)$  is individualized as:

$$G_i(t) = \sum_{j=1}^m g(t - d_{ij}) I(d_{ij} < t),$$

where  $t$  is the time since enrolment or time since the first dose, and indicates the time-varying effect of the  $j$ -th dose the  $i$ -th subject has received on the log-hazard.

### 2.2. Non-linear functions of time-varying effects

Let  $g_1(t)$  be the monotonic function proposed by Xu et al. (2017):

$$g_1(t) = Ae^{-Bt^C} + D, \text{ for } B, C > 0 \text{ and } -\infty < A, D < \infty \tag{2}$$

where  $A + D$  represents the short-term effect,  $B$  represents the rate of decay over time,  $C$  regulates the shape of the time trend, and  $D$  represents the long-term effect. If  $C = 1$  and  $D = 0$ ,  $g_1(t)$  becomes the familiar exponential decay function. A large value of  $C$  implies that the initial protection level has a duration that is quite stable before it shows a clear decline. Despite its being a non-linear function,  $g_1(t)$  has enough flexibility to capture various patterns well, including linear declines (Xu et al. 2017).

To constrain  $B$  and  $C > 0$ , the parameters are replaced by  $\exp(b)$  and  $\exp(c)$ , respectively, where  $b = \ln(B)$  and  $c = \ln(C)$ . The parameter for long-term effect,  $D$ , was proposed out of the concern of a rebound effect as discussed in the introduction.

We consider a non-monotonic function, which had its origin from a harmonic oscillator (Riley et al. 2002) and was re-parameterized by Shaw et al. (2019) for the studies of gut microbiota diversity (a continuous endpoint) before and after receiving a course of antibiotics. Let  $g_2(t)$  denotes this function:

$$g_2(t) = \frac{\alpha\beta_1\beta_2}{\beta_2 - \beta_1} (e^{-\beta_1 t} - e^{-\beta_2 t}) + \delta(1 - e^{-\beta_1 t}), \text{ for } \beta_1, \beta_2 > 0 \text{ and } -\infty < \alpha, \delta < \infty \quad (3)$$

where  $\alpha$  represents the magnitude of the initial perturbation. To constrain  $\beta_1$  and  $\beta_2 > 0$ , the parameters are replaced by  $\exp(\beta_1^*)$  and  $\exp(\beta_2^*)$ , respectively, where  $\beta_1^* = \ln(\beta_1)$  and  $\beta_2^* = \ln(\beta_2)$ . Individually,  $\beta_1$  and  $\beta_2$  do not have easy interpretations, whereas  $\varphi_1 = \beta_1 + \beta_2$  and  $\varphi_2 = \beta_1\beta_2$  represent, respectively, the damping and strength of the restoring force on the oscillator (Shaw et al. 2019). They determined the shape of the curve. Having estimated the model as parameterized in equation (3), standard errors of  $\varphi_1$  and  $\varphi_2$  can be obtained by the delta method. Finally, to allow for a long-term effect without adding too much complexity, Shaw et al. (2019) further proposed the additive term that allows a long-term effect to grow asymptotically over time to reach  $\delta$ .

Here, we derive the time to peak efficacy ( $t^*$ ) and peak level of efficacy [ $g_2(t^*)$ ]. The first derivative of  $g_2(t)$  with respect to  $t$  is:

$$\frac{\partial g_2(t)}{\partial t} = \frac{\alpha\beta_1\beta_2}{\beta_2 - \beta_1} (-\beta_1 e^{-\beta_1 t} + \beta_2 e^{-\beta_2 t}) + \beta_1 \delta e^{-\beta_1 t}.$$

Solving the equation  $\frac{\partial g_2(t)}{\partial t} = 0$  gives the time to peak efficacy,

$$t^* = \frac{1}{\beta_2 - \beta_1} \log\left(\frac{\beta_2^2}{\beta_1\beta_2 - \frac{\delta}{\alpha}(\beta_2 - \beta_1)}\right) = \frac{1}{\beta_2 - \beta_1} \log(\psi) \quad (4)$$

where

$$\psi = \frac{\beta_2^2}{\beta_1\beta_2 - \frac{\delta}{\alpha}(\beta_2 - \beta_1)}$$

Assume that there is enough time between consecutive doses such that  $t^*$  is reached before the next dose is given. Then, plugging  $t^*$  into the non-linear function  $g_2(t)$  gives a closed form expression of the peak efficacy,

$$g_2(t^*) = \frac{\alpha\beta_1\beta_2}{\beta_2 - \beta_1} \left( \psi^{-\frac{\beta_1}{\beta_2 - \beta_1}} - \psi^{-\frac{\beta_2}{\beta_2 - \beta_1}} \right) + \delta \left( 1 - \psi^{-\frac{\beta_1}{\beta_2 - \beta_1}} \right) \quad (5)$$

If  $\delta \cong 0$ , the following simplifications can be made:

$$t^* = \frac{1}{\beta_2 - \beta_1} \log\left(\frac{\beta_2}{\beta_1}\right) \quad (6)$$

$$g_2(t^*) = \frac{\alpha\beta_1\beta_2}{\beta_2 - \beta_1} \left[ \left(\frac{\beta_2}{\beta_1}\right)^{-\frac{\beta_1}{\beta_2 - \beta_1}} - \left(\frac{\beta_2}{\beta_1}\right)^{-\frac{\beta_2}{\beta_2 - \beta_1}} \right] \quad (7)$$

For intervention effects over  $m$  doses the  $i$ -th subject has received:

$$G_{hi}(t) = \sum_{j=1}^m g_h(t - d_{ij}) I(d_{ij} < t) \quad (8)$$

where  $h = 1$  or  $2$  specifies the use of the monotonic or non-monotonic function, respectively.

Furthermore, an extension of the models is to allow  $A$  in  $g_1(t)$  and  $\alpha$  in  $g_2(t)$  to be dose-specific. That is, changing  $A$  to  $A_1, A_2, \dots, A_m$  and  $\alpha$  to  $\alpha_1, \alpha_2, \dots, \alpha_m$  for the  $m$  doses in equation (8). This provides more flexibility if the cumulative dosage or intervention history modifies the efficacy profile. For example, previous research had suggested that the third dose of the Haemophilus influenzae type b vaccine appears to offer little additional benefit (Griffiths et al. 2012). The investigators may need to allow for such dose-specific effect in the statistical modelling.

### 2.3. Estimation

Let  $\theta_h$  ( $h = 1$  or  $2$ ) be the unknown parameters in equation (1), the estimators of  $\theta_h$  can be obtained by maximizing the log-partial likelihood,

$$l(\theta_h) = \sum_{i=1}^N \sum_{j=1}^{n_i} l_i(\theta_h | t_{ij})$$

$$= \sum_{i=1}^N \sum_{j=1}^{n_i} \left\{ \mathbf{y}^T \mathbf{x}_i(t_{ij}) + G_{hi}(t_{ij})z_i - \log \left( \sum_{k=1}^N Y_k(t_{ij}) \exp[\mathbf{y}^T \mathbf{x}_k(t_{ij}) + G_{hk}(t_{ij})z_k] \right) \right\},$$

where  $Y_k(t) = 1$  if the  $k$ -th subject is at risk at event time  $t$ , otherwise  $Y_k(t) = 0$ ,  $G_{hi}(t_{ij}) = \sum_{j=1}^m g_h(t_{ij} - d_{ij})I(d_{ij} < t_{ij})$  as described earlier, and  $d_{ij}$  is the time the  $i$ -th subject receives the  $j$ -th dose.

Let  $U(\theta_h) = \frac{\partial l(\theta_h)}{\partial \theta_h}$  be the score function and  $I(\theta_h) = -\frac{\partial^2 l(\theta_h)}{\partial \theta_h \partial \theta_h^T}$  be the observed information matrix;  $h = 1$  or  $2$  corresponds to the models using  $g_1(t)$  or  $g_2(t)$ , respectively. The estimators  $\hat{\theta}_1$  or  $\hat{\theta}_2$  can be obtained by solving the equations  $U(\theta_1) = 0$  or  $U(\theta_2) = 0$ . We used the quasi-Newton method (BFGS) available in the *optim* function of R (Delignette-Muller and Dutang 2021). Under regularity conditions similar to VII.2.1 and VII.2.2 in Andersen et al. (2012), it can be shown that as the sample size  $N$  tends to infinity, the estimator  $\hat{\theta}_h$  of  $\theta_h$  is consistent and asymptotically normally distributed.

Their naïve standard errors can be calculated as the square root of diagonal terms in the inverse of  $\theta_h$  or  $\theta_h$ , respectively. The AG model requires a robust sandwich estimator of variance for clustered data to deal with multiple observations per person (Cleves 1999; Lin and Wei 1989):

$$I^{-1}(\hat{\theta}_h) \sum_{i=1}^N W_i(\hat{\theta}_h) W_i^T(\hat{\theta}_h) I^{-1}(\hat{\theta}_h)$$

where

$$W_i(\hat{\theta}_h) = \sum_{j=1}^{n_i} W_i(\hat{\theta}_h | t_{ij})$$

$$= \sum_{j=1}^{n_i} \left\{ \frac{\partial l_i(\theta_h | t_{ij})}{\partial \theta_h} \Big|_{\theta_h = \hat{\theta}_h} - \sum_{k=1}^N \sum_{j'=1}^{n_k} \frac{I\{t_{ij} \geq t_{k'j'}\} \exp[\mathbf{y}^T \mathbf{x}_i(t_{k'j'}) + G_{hi}(t_{k'j'})z_i]}{\sum_{r=1}^N Y_r(t_{k'j'}) \exp[\mathbf{y}^T \mathbf{x}_r(t_{k'j'}) + G_{hr}(t_{k'j'})z_r]} \frac{\partial l_i(\theta_h | t_{k'j'})}{\partial \theta_h} \Big|_{\theta_h = \hat{\theta}_h} \right\}$$

Our analysis used this robust sandwich estimator of variance for clustered data.

## 3. A case study of intermittent preventive treatment for malaria

### 3.1. Materials and methods

We re-analyzed data from a randomized placebo-controlled trial conducted in Ghana between 2000 and 2004 for illustration (Xu et al. 2017). When the infants attended the immunization clinic at the age of about 2 months for a dose of diphtheria-pertussis-tetanus vaccine, they were enrolled and

randomized to receive placebo or sulfadoxine-pyrimethamine (SP) for malaria prevention. Four doses of SP or placebo were scheduled over a duration of 9 months, at 1, 2, 7 and 10 months after enrolment. The schedule was designed such that the dosing coincided with the time the infants would visit the health care facilities for vaccination. There was substantial individual variation in the actual timing of the administration of SP/placebo, with mean (SD) of the first to fourth doses at 1.03 (0.33), 2.11 (0.52), 7.60 (0.87) and 10.75 (0.98) months after enrolment, respectively. The infants were monitored for up to 24 months. The primary endpoint, clinical malaria, was defined as a visit to a health care facility with malaria parasites in the blood confirmed by microscopy and temperature  $\theta_h$  or a parental report of fever. To avoid double-counting, malaria cases recorded within 7 days of a previous malaria episode in the same person were ignored (Xu et al. 2017). Approximately 90% of the infants completed the full follow-up; 2045 infants received all four doses of SP/placebo. In total, there were 1442 malaria episodes among 1044 infants in the SP group, and 1593 malaria episodes among 1001 infants in the placebo group.

We set the origin of analysis time ( $t = 0$ ) to be the date of receiving the first dose of SP or placebo for each infant. The covariates included in all models were age (at enrolment) and season (July to November was rainy season; dry season otherwise). Age is a time-constant while season is a time-varying covariate.

We first fitted the AG model with the intervention group versus placebo group as a time-constant exposure variable, i.e. a PH model. Then, we replaced the time-constant intervention group versus placebo group variable by either  $G_1(t)$  or  $G_2(t)$  to capture the time-varying effects of the four doses of SP. For each model, we computed the Akaike Information Criterion (AIC) and Bayesian Information Criterion (BIC) (Royston and Lambert 2011). BIC imposes heavier penalty on model complexity (number of parameters) than AIC. Since  $G_1(t)$  and  $G_2(t)$  have the same complexity, the results on comparison between them are expected to agree. To compare models with the same  $A$  or  $\alpha$  across doses versus models with dose-specific  $A_m$  or  $\alpha_m$ , we considered both AIC and BIC.

To challenge the performance of the 4-parameter functions, we fitted a model with  $g(t)$  being a step function with eight steps (weeks 1, 2, 3, 4, 5–6, 7–8, 9–12 and  $\geq 13$ ), and a series of models with  $g(t)$  represented by cubic B-splines. A cubic B-spline with 1 (inner) knot has the same complexity as  $g_1(t)$  or  $g_2(t)$ , i.e. four coefficients to be estimated (Perperoglou et al. 2019). We consider cubic B-spline models with 1 to 4 knots. While the location of knots usually has limited impact to the model fit (Durrleman and Simon 1989; Royston and Lambert 2011), it is appropriate to place them where flexibility is needed (Wei et al. 2006). Previous studies of SP have suggested that its efficacy tends to be limited within a duration of about 4 to 6 weeks (Akbari et al. 2012; Cairns et al. 2008). Placing knots beyond this time frame is unnecessary. We fitted five 1-knot models, with the knots at 7, 14, 21, 28 or 35 days since dosing, four 2-knot models, at (5, 20), (7, 21), (7, 28), or (14, 28) days, two 3-knot models, at (5, 15, 30) or (7, 21, 35) days, and one 4-knot models, at (5, 15, 25, 40). For each set of spline models with the same number of knots, we compared the AIC of the best fitting spline model (smallest AIC) and step function model with that of the models using the 4-parameter functions.

The fitting of multiple spline models with knots at multiple sets of location increases the risk of over-fitting. It was used here only for the purpose of challenging the performance of the 4-parameter functions.

Note that the model formulation assumed that the long-term, rebound effect, if any, accumulates over doses. To explore whether the assumption of cumulative rebound effect was valid, we further estimated an AG model that included only the follow-up time from 3 months after receiving the second dose of SP/placebo till the third dose (period 1) and the follow-up time from 3 months after receiving the fourth (last) dose of SP/placebo till the end of follow-up (period 2). One AG model is fitted, with two terms to estimate the effects of SP group versus placebo group in period 1 and in period 2 (i.e. allowing interaction between group and time-period) and two terms to control for age and season. The focus on these two

time-periods was motivated by (a) the longer spacing between the second and third dose in this trial and (b) the likely disappearance of the short-term SP effect by 3 months after dosing. That is, these are the time-periods that likely showed only the long-term effect. The HR estimates for the two periods were compared with each other and with the model estimates based on  $G_1(t)$  and  $G_2(t)$ .

### 3.2. Results

The PH model gave AIC 44613.01 and BIC 44631.06 (Table 1). Infants in the SP group was estimated to have an HR of  $\exp(-0.138) = 0.871$  as compared to the placebo group.

The models with monotonic and non-monotonic function,  $G_1(t)$  and  $G_2(t)$ , using the same  $A$  or  $\alpha$  across doses, gave smaller AIC and BIC than the PH model (Table 1). Clearly, the PH model was less adequate and the time-constant effect assumption was not tenable. Both AIC and BIC indicated the superiority of  $G_2(t)$  over  $G_1(t)$  for this dataset. Allowing dose-specific  $A_m$  or  $\alpha_m$ , i.e. using three more parameters in each of the respective models, led to larger AIC and BIC than the model with a constant  $A$  or  $\alpha$ . So, we focused on the simple 4-parameter functions.

The AIC and BIC of the step function model and the best fitting models within each set of spline models with the same number of knots are also shown in Table 1. (Results for all the spline models fitted are shown in Appendix 1.) According to both AIC and BIC,  $G_2(t)$  fitted the data best. According to BIC,  $G_1(t)$  was the second best. According to AIC, which imposed less penalty on model complexity, the step function was the second best. We focused on these top three models in further discussion.

Table 2 shows the regression coefficient estimates for the monotonic and non-monotonic function models. Based on the estimates, we plotted the estimated time-varying HR in Figure 1. The estimated step function was also included in the figure. The graphing assumed that the four doses were received at 0, 1, 6 and 9 months (from dose 1) as scheduled. From the figure, it can be seen that the three series of estimates show approximately the same pattern. The main difference between them is in the first 3 weeks after dosing, where  $G_1(t)$  deviates from the other two.

In the model using the monotonic function  $G_1(t)$ , the short-term effect in terms of HR is  $\exp(A + D) = \exp(-1.504 + 0.022) = 0.227$  (95% confidence interval, CI, 0.168 to 0.307). This high level of efficacy was maintained for about half a month, and then the HR changed sharply towards zero.

**Table 1.** Akaike Information Criterion (AIC) and Bayesian Information Criterion (BIC) of Andersen–Gill models with time-constant intervention effect (proportional hazard, PH), monotonic function [ $G_1(t)$ ], non-monotonic function [ $G_2(t)$ ], step function (Step) and cubic B-splines with 1 to 4 knots (Spline 1 to Spline 4).<sup>\*</sup>

	PH	$G_1(t)$	$G_2(t)$	Models Step <sup>†</sup>	Spline 1 <sup>‡</sup>	Spline 2 <sup>‡</sup>	Spline 3 <sup>‡</sup>	Spline 4 <sup>‡</sup>
AIC	44613.01	44433.90	44389.71	44421.07	44526.69	44511.96	44510.11	44511.75
BIC	44631.06	44473.02	44428.83	44481.25	44562.80	44554.09	44558.26	44565.91

<sup>\*</sup> All models adjusted for age and season.

<sup>†</sup> HR varied between eight time-intervals (weeks 1, 2, 3, 4, 5–6, 7–8, 9–12 and  $\geq 13$ ).

<sup>‡</sup> For each cubic B-spline model with  $k$  knots ( $k = 1, 2, 3$  or  $4$ ), several models with the  $k$  knots placed at different locations were fitted (see text for details). The table shows the results of the spline model that has the smallest AIC among all models with the same number of knots.

**Table 2.** Analyses using the AG model with  $G_1(t)$  and  $G_2(t)$ .

Parameter	Model with $G_1(t)$		Parameter	Model with $G_2(t)$	
	Estimate	SE		Estimate	SE
A	-1.504	0.155	$\alpha$	-2.106	0.168
ln(B)	-0.926	0.318	$\ln(\varphi_1)$	1.828	0.128
ln(C)	1.354	0.287	$\ln(\varphi_2)$	2.258	0.079
D	0.022	0.013	$\delta$	0.027	0.013
Age	0.108	0.040	Age	0.107	0.040
Season	1.512	0.044	Season	1.512	0.044



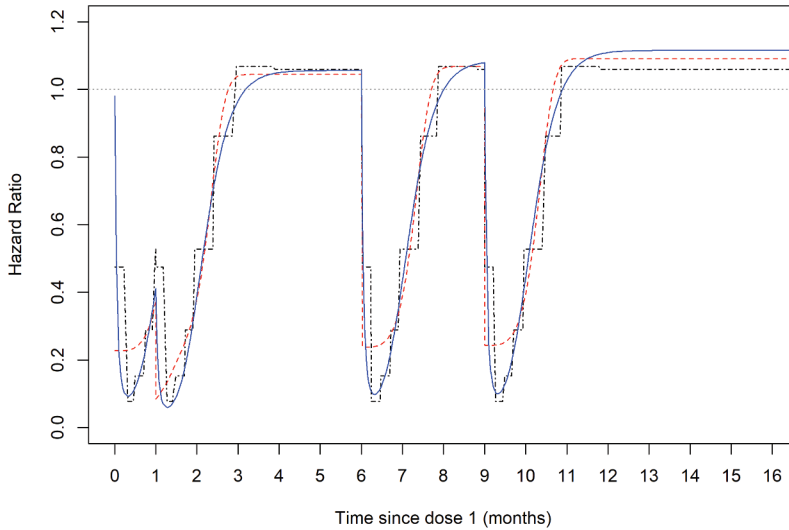


**Figure 1.** Estimated time-varying hazard ratios, assuming the timing of dosing were at 0, 1, 6 and 9 months as scheduled. Dashed line (red):  $G_1(t)$ ; solid line (blue):  $G_2(t)$ ; dot-dashed line (black): step function; dotted (grey) reference line at HR = 1.

**Table 3.** Analysis of long-term effect in period 1 (3 months after dose 2 till dose 3) and period 2 (3 months after dose 4).

Exposure	Hazard Ratio	95% CI
SP group, period 1	1.069	[0.893, 1.280]
SP group, period 2	1.106	[0.984, 1.243]
Age	1.095	[1.006, 1.191]
Season	4.634	[4.109, 5.225]

In contrast, the estimates for the model with non-monotonic function indicate that it took about  $t^* = 0.321$  months ( $\sim 10$  days) after dosing to reach the peak protective efficacy level, at  $HR = 0.093$ , according to equations (6) and (7). The HR's estimated by the model with step function for weeks 1, 2, 3, 4, 5–6, 7–8, 9–12 and  $\geq 13$  were 0.475, 0.077, 0.153, 0.289, 0.528, 0.862, 1.068 and 1.059, respectively.

All three models showed a small rebound effect. The HR's for the models with monotonic and non-monotonic functions were  $HR = \exp(0.022) = 1.022$  (0.997 to 1.048) and  $\exp(0.027) = 1.027$  (1.002 to 1.054), respectively. The HR for the last step of the step function was 1.059 (0.971 to 1.156) as aforementioned. Table 3 shows the results of further analyses that used only the data from the time-periods of 3-month after dose 2 till dose 3 and 3-month after dose 4 till end of follow-up. The estimated HR's for SP were 1.069 in the first and 1.106 in the second period (test for SP-by-period interaction,  $P = .76$ ). While there was no statistically significant level of rebound effect or interaction, the point estimates gave some support to the model assumption that the long-term rebound effect accumulated over doses. In comparison, the estimates of rebound effect over two doses obtained from the monotonic, non-monotonic and step functions were  $1.022^2 = 1.044$ ,  $1.027^2 = 1.055$ , and  $1.059^2 = 1.121$ , respectively. Over four doses, the rebound effect estimated by the monotonic, non-monotonic and step functions were 1.092, 1.116, and 1.258, respectively. The non-monotonic function showed more agreement than the other two functions with the period-specific estimates in Table 3.

If we used protective efficacy dropping from peak level to half of the peak level as indicative of the appropriate time-point for re-administration of the product,  $g_1(t)$  and  $g_2(t)$  indicate that the timing was about 37 days and 35 days since the previous dose, respectively. The step function suggested the timing to be about 5–6 weeks since the previous dose.

## 4. Simulation

### 4.1. Methods

We evaluated the point and interval estimation of the proposed non-monotonic model by simulation. We considered four patterns of protective efficacy defined by  $\alpha, \beta_1^*, \beta_2^*, \delta$ :

Pattern 1 = (-2,1,1.5,0)

Pattern 2 = (-2,1,1.5,0.1)

Pattern 3 = (-2,0.5,1,0)

Pattern 4 = (-2,0.5,1,0.1)

All patterns had the same initial perturbation ( $\alpha = -2$ ). Patterns 1 and 2 had earlier peak and sharper decline over time than patterns 3 and 4. Patterns 1 and 3 had no rebound effects ( $\delta = 0$ ) while patterns 2 and 4 did. We considered intervention schedules with a single dose, two doses and three doses, with intervals between doses in the two and three dose schedules independently following a Uniform(2,3) distribution. For each set of parameters, we simulated large, medium and small sample sizes (1300, 1000 and 700 persons per trial arm, respectively). There were  $4 \times 3 \times 3 = 36$  scenarios in total. The incidence level was set such that the scenarios with 1000 persons per trial arm resembled the case study of malaria chemoprevention not only in terms of number of persons per trial arm but also number of events in the control arm (about 1500 events). Further details of the simulation procedures are available in [Appendix 2](#). For each scenario, we evaluated the relative bias of the estimator, ratio of mean standard errors to empirical standard deviation of estimates, and coverage probability of the 95% CI of the estimates of  $\alpha, \varphi_1, \varphi_2$  and  $\delta$ . For patterns 1 and 3 where there was no long-term effect ( $\delta = 0$ ), we evaluated the absolute bias of the estimator for  $\delta$  because the use of relative bias would involve division by zero. Furthermore, we derived the time-to-peak PE and peak PE level from the parameter estimates using equations 4 and 5, and present the mean ratio of time-to-peak PE and peak PE level to their respective true values as determined by the true model parameter values.

### 4.2. Results

[Table 4](#) shows the simulation results on the estimation of model parameters. The key finding is that the proposed method worked well when, similar to the case study of malaria prevention, sample size was large or the intervention consisted of multiple doses. Conversely, the bias level was raised and coverage probability of confidence intervals was below target level when sample size was smaller, especially if there was only one single dose.

Across all four patterns of PE, when sample size was 1300 and number of intervention doses was three, relative bias in the estimation of the four parameters was small, ranging from 1.2% to 3.6%. Absolute bias in the estimation of  $\delta$  (when true  $\delta = 0$ ) was no more than 0.004. The ratios of average standard error to empirical standard deviation were close to one; the 95% CIs had coverage probability close to the target level. Among the scenarios with three doses of intervention, varying the sample size from 1300 to 1000 or 700 did not make much impact on these properties. In the scenarios of two doses and sample size = 1000 or 1300, the performance of the method was similar to the aforementioned. In the scenarios of one dose only and in the scenarios of two doses and sample size was 700 only, except for the parameter  $\delta$ , there was more visible elevation of relative bias, under-estimation of standard error, and in some cases (one dose and  $N = 700$ ) coverage probability of 95% CIs dropped to about 90% only.

**Table 4.** Simulation results, by number of doses, sample size and PE patterns.<sup>\*,†</sup>

(Dose; N; pattern)	$\alpha$			$\ln(\varphi_1)$			$\ln(\varphi_2)$			$\delta$		
	Bias (%)	ASE/ESD	CP (%)	Bias (%)	ASE/ESD	CP (%)	Bias (%)	ASE/ESD	CP (%)	Bias (%)	ASE/ESD	CP (%)
(3; 1300; 1)	2.5	1.05	95.4	3.0	0.99	93.0	1.6	1.02	96.4	0.003 <sup>†</sup>	1.00	94.4
(3; 1300; 2)	2.2	1.07	96.0	2.5	1.02	92.6	1.2	1.02	95.6	2.3	1.00	94.8
(3; 1300; 3)	2.4	1.07	96.0	3.6	1.01	95.2	1.8	1.01	95.6	0.004 <sup>†</sup>	1.05	95.0
(3; 1300; 4)	2.1	1.07	95.6	3.4	0.98	93.8	1.8	0.99	95.6	3.6	1.00	95.0
(3; 1000; 1)	1.6	1.02	95.4	4.0	0.96	94.6	2.6	1.04	95.6	0.004 <sup>†</sup>	1.00	95.4
(3; 1000; 2)	1.5	1.02	95.8	3.6	0.96	93.4	2.4	1.05	95.0	3.0	1.00	95.6
(3; 1000; 3)	2.0	1.01	93.6	5.8	0.97	95.2	3.8	1.03	95.8	0.005 <sup>†</sup>	1.00	95.0
(3; 1000; 4)	1.3	1.03	94.2	5.2	0.99	95.6	3.6	1.02	96.8	4.3	1.00	94.8
(3; 700; 1)	3.1	0.97	94.2	3.9	1.07	94.4	1.8	1.04	95.2	0.005 <sup>†</sup>	1.00	95.6
(3; 700; 2)	3.5	0.96	94.6	3.7	0.99	93.8	1.9	1.00	94.4	3.5	0.96	94.6
(3; 700; 3)	4.0	1.06	94.4	5.2	1.11	95.8	2.2	1.07	96.8	0.007 <sup>†</sup>	1.04	96.0
(3; 700; 4)	3.2	1.00	94.2	4.5	1.01	95.6	1.7	1.05	96.4	6.0	1.04	95.0
(2; 1300; 1)	2.5	1.02	96.0	4.1	1.01	95.2	2.6	1.04	95.3	0.002 <sup>†</sup>	1.00	95.2
(2; 1300; 2)	2.4	1.01	96.0	3.9	1.04	96.2	2.5	1.05	95.6	1.9	1.00	94.2
(2; 1300; 3)	2.2	1.06	96.0	5.6	1.02	95.6	3.6	1.06	96.6	0.003 <sup>†</sup>	0.96	93.8
(2; 1300; 4)	1.9	1.05	95.4	5.6	1.00	94.6	3.8	1.04	95.4	3.0	0.96	94.0
(2; 1000; 1)	1.9	0.97	93.8	5.0	0.95	94.4	3.4	1.03	95.2	0.004 <sup>†</sup>	0.96	93.6
(2; 1000; 2)	1.9	0.99	94.8	5.2	0.99	94.2	3.5	1.05	95.8	3.7	1.00	94.2
(2; 1000; 3)	2.1	0.98	94.4	8.1	0.88	93.8	5.8	0.95	95.6	0.005 <sup>†</sup>	0.96	93.0
(2; 1000; 4)	1.5	0.98	93.6	7.4	0.95	94.8	5.5	1.03	96.6	4.8	0.96	92.2
(2; 700; 1)	3.8	0.98	96.0	6.1	0.82	92.4	3.6	0.85	93.8	0.003 <sup>†</sup>	1.00	94.0
(2; 700; 2)	3.6	0.97	95.2	6.0	0.81	93.0	3.8	0.85	93.8	2.9	0.96	95.2
(2; 700; 3)	3.7	1.02	94.6	7.3	0.96	94.2	4.6	0.94	96.2	0.004 <sup>†</sup>	1.00	94.4
(2; 700; 4)	3.2	1.00	95.0	6.8	0.91	94.2	4.3	0.94	95.6	4.5	1.00	94.6
(1; 1300; 1)	4.5	0.99	93.8	8.0	0.70	92.4	5.3	0.77	93.0	0.003 <sup>†</sup>	0.97	94.6
(1; 1300; 2)	4.3	0.96	93.2	7.3	0.82	91.8	4.8	0.89	93.4	3.7	0.97	95.0
(1; 1300; 3)	4.4	1.02	94.4	9.2	0.91	92.2	6.3	0.96	93.4	0.006 <sup>†</sup>	0.98	95.4
(1; 1300; 4)	3.8	1.01	94.2	8.9	0.93	93.2	6.4	0.99	94.0	5.4	0.98	94.0
(1; 1000; 1)	4.7	1.00	95.6	10.6	0.82	92.6	7.4	0.85	91.4	0.008 <sup>†</sup>	1.00	94.2
(1; 1000; 2)	4.7	1.00	96.6	10.0	0.72	91.8	6.9	0.76	91.8	7.5	0.98	94.6
(1; 1000; 3)	5.2	0.99	95.0	15.1	0.64	92.8	11.3	0.70	93.4	0.011 <sup>†</sup>	0.98	94.2
(1; 1000; 4)	4.3	0.98	94.4	14.3	0.72	92.4	11.0	0.77	93.6	10.4	1.00	94.2
(1; 700; 1)	7.5	0.94	95.8	13.4	0.59	91.2	9.0	0.63	90.0	0.005 <sup>†</sup>	1.02	95.6
(1; 700; 2)	6.9	0.93	96.4	12.8	0.57	90.4	8.8	0.60	90.8	4.9	1.00	95.0
(1; 700; 3)	7.1	1.02	94.8	17.4	0.48	89.4	13.5	0.54	90.6	0.008 <sup>†</sup>	1.00	94.6
(1; 700; 4)	6.4	1.00	94.0	17.1	0.49	90.4	13.5	0.54	90.8	7.7	1.00	94.6

\*Bias is relative bias in percent (except for  $\delta$  in patterns 1 and 3); ASE/ESD is ratio of mean standard error to empirical standard deviation of estimates; CP is coverage probability of 95% confidence interval in percent.

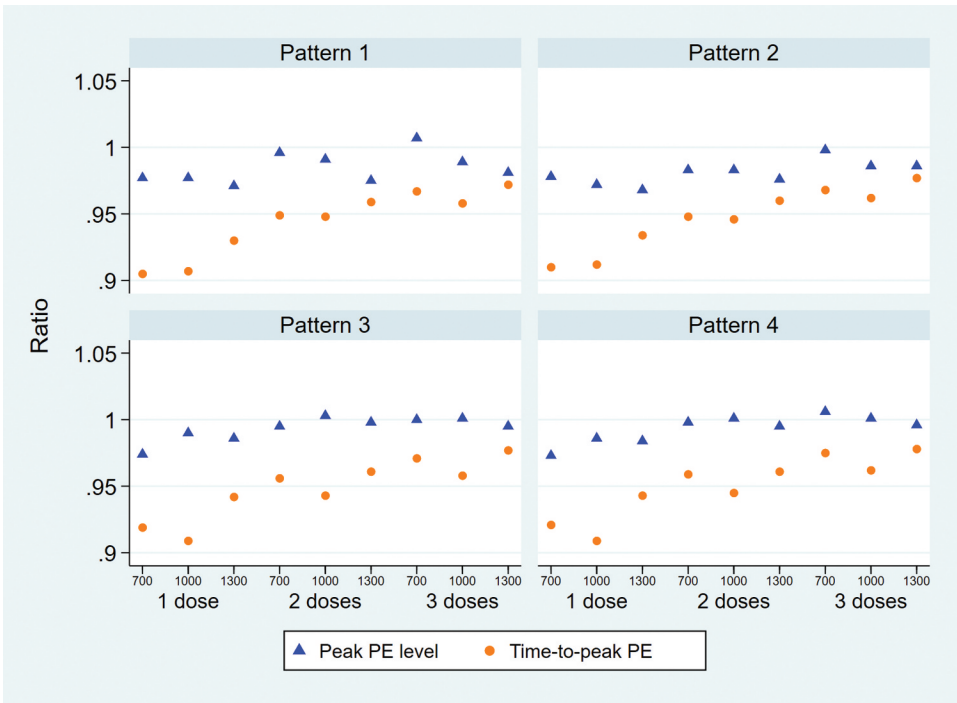
<sup>†</sup>Absolute bias in the estimation of  $\delta$  when true  $\delta = 0$  (patterns 1 and 3).

Figure 2 shows the mean ratio of peak PE level and mean ratio of time-to-peak PE to their respective true values, by pattern of PE, sample size and number of doses. The mean ratio of peak PE level was close to one across all the settings evaluated. The mean ratio of time-to-peak PE was mostly close to one, but it declined as sample size or number of doses decreased. It dropped to about 0.9 in scenarios with only one dose and  $N = 700$  or  $1000$ .

## 5. Discussion

Knowledge on the level of protective efficacy over time is important in the evaluation and deployment of interventions against infectious diseases. The time pattern of protective efficacy may be affected by local level of disease transmission intensity and drug resistance (Cheung et al. 2020; White 2005). It is useful to assess and monitor the pattern not only during product development but also in post-licensure surveillance where the products are deployed.

Recently, Xu et al. (2017) proposed a 4-parameter monotonic function for modelling the waning of protective efficacy in recurrent event times, allowing individual variation in the timing of dosing. We consider an alternative, using the same number of parameters but allowing for non-monotonic trend. We derived the expressions for time-to-peak efficacy and level of peak efficacy.



**Figure 2.** Mean ratios of peak PE level (triangle) and time-to-peak PE (dot) to their respective true values, by pattern of PE, sample size and number of doses.

In the case study of intermittent prevention treatment for malaria, the model with the 4-parameter non-monotonic function outperformed models with the 4-parameter monotonic function. In this dataset, we subjected it to the challenges of multiple models based on spline or step functions. The non-monotonic function remained the best fitting.

Simulations showed that the method worked well for studies that had sample sizes and number of doses similar to or larger than the case study of malaria prevention. For studies with smaller sample sizes and only one single dose, the estimation was not accurate. Researchers will need to be aware of the limitation when choosing to use the method.

It is conceivable that the cumulative dose history may affect efficacy level. Therefore, we explored the models that allow dose-specific  $A_m$  or  $\alpha_m$ . In this study of SP, the timing of doses was planned such that the dosing coincided with visits for the Expanded Program on Immunization. The doses were therefore quite separated over time. The effect of the latest dose might have mostly dissipated before the next dose was given. This may explain the lack of better fit when the additional parameters were introduced. We postulate that the more complex models may have better performance in situations that doses are given closer in time.

Following the previous study (Xu et al. 2017), in  $g_1(t)$  the parameter  $D$  is constant over time, making  $A + D$  the short-term effect. In light of the asymptotically growing long-term effect in  $g_2(t)$ , an adaption can be made in  $g_1(t)$ , replacing  $D$  by  $D[1 - \exp(-B \times t)]$ , such that  $A$  alone is the short-term effect. However, given that  $D$  was a very small and statistically non-significant value in the malaria study, we did not consider the additional work.

Our model formulation allows the long-term effect to accumulate over time, such that after  $m$  doses the long-term effect in terms of HR becomes  $\exp(m \times \text{coefficient})$  for the two parametric functions. For clinical trials that involve multiple doses of intervention and have relatively short follow-up periods, this appears a reasonable formulation. Data from the malaria study were also consistent with it.

However, if  $m$  doses are spread over a long duration such that any effect of the previous dose could have mostly dissipated, further modification of the functions may be considered.

## Data availability statement

Data sharing is not applicable to this article as no new data were created or analyzed in this study.

## Disclaimer

Any opinions, findings and conclusions or recommendations expressed in this material are those of the authors and do not reflect the views of Ministry of Health/National Medical Research Council, Singapore.

## Disclosure statement

No potential conflict of interest was reported by the author(s).

## Funding

This work was supported by the National Medical Research Council, Singapore (MOH-000526).

## ORCID

Yin Bun Cheung  <http://orcid.org/0000-0003-0517-7625>

Xiangmei Ma  <http://orcid.org/0000-0001-6526-1226>

K. F. Lam  <http://orcid.org/0000-0001-5453-994X>

Chee Fu Yung  <http://orcid.org/0000-0001-9605-7690>

Paul Milligan  <http://orcid.org/0000-0003-3430-3395>

## References

- Akbari, S., N. Y. Valdy, and L. M. Wahl. 2012. The time distribution of sulfadoxine-pyrimethamine protection from malaria. *Bulletin of Mathematical Biology* 74 (11):2733–2751. doi:10.1007/s11538-012-9775-4.
- Andersen, P. K., O. Borgan, R. D. Gill, and N. Keiding. 2012. *Statistical models based on counting processes*. Stockholm: Springer.
- Cairns, M., I. Carneiro, P. Milligan, S. Owusu-Agyei, T. Awine, R. Gosling, B. Greenwood, and D. Chandramohan. 2008. Duration of protection against malaria and anaemia provided by intermittent preventive treatment in infants in Navrongo, Ghana. *PLoS One* 3 (5):e2227. doi:10.1371/journal.pone.0002227.
- Cheung, Y. B., P. S. F. Yip, and J. P. E. Karlberg. 2001. Parametric modeling of neonatal mortality in relation to size at birth. *Statistics in Medicine* 20 (16):2455–2466. doi:10.1002/sim.858.
- Cheung, Y. B., Y. Xu, S. H. Tan, F. Cutts, and P. Milligan. 2010. Estimation of intervention effects using first or multiple episodes in clinical trials: The Andersen-Gill model re-examined. *Statistics in Medicine* 29 (3):328–333. doi:10.1002/sim.3783.
- Cheung, Y. B., X. Ma, K. F. Lam, and P. Milligan. 2020. Estimation of the primary, secondary and composite effects of malaria vaccines using data on multiple clinical malaria episodes. *Vaccine* 38 (32):4964–4969. doi:10.1016/j.vaccine.2020.05.086.
- Cleves, M. 1999. Analysis of multiple failure-time data with Stata. *Stata Technical Bulletin* 49:30–39.
- Cutts, F. T., S. M. Zaman, G. Enwere, S. Jaffar, O. S. Levine, J. B. Okoko, C. Oluwalana, A. Vaughan, S. K. Obaro, A. Leach, et al. 2005. Efficacy of nine-valent pneumococcal conjugate vaccine against pneumonia and invasive pneumococcal disease in the Gambia: Randomised, doubled-blind, placebo-controlled trial. *The Lancet* 365 (9465):1139–1146. doi:10.1016/S0140-6736(05)71876-6.
- Delignette-Muller, M. L., and C. Dutang. 2021. Which optimization algorithm to choose? Accessed February 19, 2022. <https://cran.r-project.org/web/packages/fitdistrplus/vignettes/Optimalgo.html>.
- Durrleman, S., and R. Simon. 1989. Flexible regression models with cubic splines. *Statistics in Medicine* 8 (5):551–561. doi:10.1002/sim.4780080504.
- European Medicines Agency. 2020. *Qualification opinion of clinically interpretable treatment effect measures based on recurrent event endpoints that allow for efficient statistical analysis*. Amsterdam: EMA.

- Griffiths, U. K., A. Clark, B. Gessner, A. Miners, C. Sanderson, E. R. Sedyaningsih, and K. E. Mulholland. 2012. Dose-specific efficacy of Haemophilus influenzae type b conjugate vaccines: A systematic review and meta-analysis of controlled clinical trials. *Epidemiology and Infection* 140 (8):1343–1355. doi:10.1017/S0950268812000957.
- Grobusch, M. P., J. J. Gabor, J. J. Apointe, N. G. Schwarz, M. Poetschke, J. Doernemann, K. Schuster, K. B. Koester, K. Profanter, L. B. Borchert, et al. 2009. No rebound of morbidity following intermittent preventive sulfadoxine-pyrimethamine treatment of malaria in infants in Gabon. *Journal of Infectious Diseases* 200 (11):1658–1661. doi:10.1086/647990.
- Jahn-Eimermacher, A., K. Ingel, S. Preussler, A. Bayes-Genis, and H. Binder. 2017. A DAG-based comparison of intervention effect underestimation between composite endpoint and multi-state analysis in cardiovascular trials. *BMC Medical Research Methodology* 17 (1):92. doi:10.1186/s12874-017-0366-9.
- Kanaan, M. N., and C. P. Farrington. 2002. Farrington. Estimation of waning vaccine efficacy. *Journal of American Statistical Association* 97 (458):389–397. doi:10.1198/016214502760046943.
- Kelly, P. J., and L. L. Lim. 2000. Survival analysis for recurrent event data: An application to childhood infectious diseases. *Statistics in Medicine* 19 (1):13–33. doi:10.1002/(sici)1097-0258(20000115)19:1<13::aid-sim279>3.0.co;2-5.
- Lin, D. Y., and L. J. Wei. 1989. The robust inference for the Cox proportional hazards model. *Journal of the American Statistical Association* 84 (408):1074–1078. doi:10.1080/01621459.1989.10478874.
- Lopez Bernal, J., N. Andrews, C. Gower, C. Robertson, J. Stowe, E. Tessier, R. Simmons, S. Cottrell, R. Roberts, M. O'Doherty, et al. 2021. Effectiveness of the Pfizer-BioNTech and Oxford-AstraZeneca vaccines on Covid-19 related symptoms, hospital admissions, and mortality in older adults in England: Test negative case-control study. *BMJ* 373:n1088. doi:10.1136/bmj.n1088.
- Metcalfe, C., and S. G. Thompson. 2007. Wei, Lin and Weissfeld's marginal analysis of multivariate failure time data: Should it be applied to a recurrent events outcome? *Statistical Methods in Medical Research* 16 (2):103–122. doi:10.1177/0962280206071926.
- Moghadas, S. M., T. N. Vilches, K. Zhang, S. Nourbakhsh, P. S. Meagan, M. C. Fitzpatrick, and A. P. Galvani. 2021. Evaluation of COVID-19 vaccination strategies with a delayed second dose. *PLoS Biology* 19 (4):e3001211. doi:10.1371/journal.pbio.3001211.
- Moorthy, V. S., Z. Reed, and P. G. Smith. WHO Malaria Vaccine Advisory Committee. 2009. MALVAC 2008: Measures of efficacy of malaria vaccines in phase 2b and phase 3 trials—scientific, regulatory and public health perspectives. *Vaccine* 27 (5):624–628. doi:10.1016/j.vaccine.2008.
- Nahlen, B. L., J. P. Clark, and D. Alnwick. 2003. Insecticide-treated bednets. *American Journal of Tropical Medicine & Hygiene* 68 (4 Suppl):1–2. doi:10.4269/ajtmh.2003.68.1.
- Odhiambo, F. O., M. J. Hamel, J. Williamson, K. Lindblade, F. O. ter Kuile, E. Peterson, P. Otieno, S. Kariuki, J. Vulule, L. Slutsker, et al. 2010. Intermittent preventive treatment in infants for the prevention of malaria in rural Western Kenya: A randomized, double-blind placebo-controlled trial. *PLoS One* 5 (4):e10016. doi:10.1371/journal.pone.0010016.
- Perperoglou, A., W. Sauerbrei, M. Abrahamowicz, and M. Schmid. Schmid, and TG2 of the STRATOS Initiative. 2019. A review of spline function procedures in R. *BMC Medical Research Methodology* 19 (1):46. doi:10.1186/s12874-019-0666-3.
- Phiri, M. D., M. Cairns, I. Zongo, F. Nikiema, M. Diarra, R. S. Yerbanga, A. Barry, A. Tapily, S. Coumare, I. Theria, et al. 2021. The duration of protection from azithromycin against malaria, acute respiratory, gastrointestinal, and skin infections when given alongside seasonal malaria chemoprevention: Secondary analyses of data from a clinical trial in Houndé, Burkina Faso, and Bougouni, Mali. *Clinical Infectious Diseases* 73 (7):e2379–e2386. doi:10.1093/cid/ciaa1905.
- Porco, T. C., J. Hart, A. M. Arzika, J. Weaver, K. Kalua, Z. Mrango, S. Y. Cotter, N. E. Stoller, K. S. O'Brien, D. M. Fry, et al. 2019. Mass oral azithromycin for childhood mortality: Timing of death after distribution in the MORDOR trial. *Clinical Infectious Diseases* 68 (12):2114–2116. doi:10.1093/cid/ciy973.
- Rauch, G., M. Kieser, H. Binder, A. Bayes-Genis, and A. Jahn-Eimermacher. 2018. Time-to-first-event versus recurrent-event analysis: Points to consider for selecting a meaningful analysis strategy in clinical trials with composite endpoints. *Clinical Research in Cardiology* 107 (5):437–443. doi:10.1007/s00392-018-1205-7.
- Riley, K. F., M. P. Hobson, and S. J. Bence. 2002. Eigenfunction methods for differential equations. In K. F. Riley, M. P. Hobson, and S. J. Bence (Eds.), *Mathematical Methods for Physics and Engineering*, Vol. 2nd, pp. 581–607. Cambridge: Cambridge U. P.
- Royston, P., and P. C. Lambert. 2011. *Flexible parametric survival analysis using stata: Beyond the cox model*. College Station, Tx: Stata Press.
- RTS,S Clinical Trials Partnership. 2015. Efficacy and safety of RTS,S/AS01 malaria vaccine with or without a booster dose in infants and children in Africa: Final results of a phase 3, individually randomised, controlled trial. *The Lancet* 386 (9988):31–45. doi:10.1016/S0140-6736(15)60721-8.
- Shaw, L. P., H. Bassam, C. P. Barnes, A. S. Walker, N. Klein, and F. Balloux. 2019. Modelling microbiome recovery after antibiotics using a stability landscape framework. *The ISME Journal* 13 (7):1845–1856. doi:10.1038/s41396-019-0392-1.
- Skowronski, D. M., and G. De Serres. 2021. Safety and efficacy of the BNT162b2 mRNA Covid-19 vaccine. *New England Journal of Medicine* 384 (16):1576–1577. doi:10.1056/NEJMc2036242.
- Smith, P. G., and P. Milligan. 2005. Malaria vaccine: 3 or 6 months' protection? *Lancet* 365 (9458):472–473. doi:10.1016/S0140-6736(05)17860-X.

- Voysey, M., S. A. C. Clemens, S. A. Madhi, L. Y. Weckx, P. M. Folegatti, P. K. Aley, B. Angus, V. L. Baillie, S. L. Barnabas, Q. E. Bhorat, et al. 2021. Single-dose administration and the influence of the timing of the booster dose on immunogenicity and efficacy of ChAdOx1 nCoV-19 (AZD222) vaccine: A pooled analysis of four randomised trials. *Lancet* 397 (10277):881–891. doi:10.1016/S0140-6736(21)00432-3.
- Wei, Y., A. Pere, R. Koenker, and X. He. 2006. Quantile regression methods for reference growth charts. *Statistics in Medicine* 25 (8):1369–1382. doi:10.1002/sim.2271.
- White, N. J. 2005. Intermittent presumptive treatment for malaria. *PLoS Medicine* 2 (1):e3. doi:10.1371/journal.pmed.0020003.
- Xu, Y., Y. B. Cheung, K. F. Lam, and P. Milligan. 2012. Estimation of summary protective efficacy using a frailty mixture model for recurrent event time data. *Statistics in Medicine* 31 (29):4023–4039. doi:10.1002/sim.5458.
- Xu, J., K. F. Lam, F. Chen, P. Milligan, and Y. B. Cheung. 2017. Semiparametric estimation of time-varying intervention effects using recurrent event data. *Statistics in Medicine* 36 (17):2682–2696. doi:10.1002/sim.7319.

## Appendix 1

**Table A1.** Akaike Information Criterion and Bayesian Information Criterion of AG models with cubic B-spline models with 1 to 4 knots.\*

Number of knots	Knot locations	AIC	BIC
1	7	44530.29	44566.40
1	14	44529.72	44565.83
1	21	44528.78	44564.89
1	28	44527.74	44563.85
1	35	44526.69	44562.80
2	5, 20	44511.96	44511.96
2	7, 21	44516.19	44558.31
2	7, 28	44516.28	44558.41
2	14, 28	44515.10	44557.22
3	5, 15, 30	44510.11	44558.26
3	7, 21, 35	44513.05	44561.19
4	5, 15, 25, 40	44511.75	44565.91

\*Adjusted for age and season.

## Appendix 2. Simulation procedures

Since the model involved the time-dependent hazard function, we used the thinning approach for generation of the recurrent event times (Xu et al. 2017). For the  $i$ -th subject, generate recurrent event time  $t_{ij}$  ( $j = 1, 2, \dots$ ) in months from a model  $\lambda_i(t) = \lambda_0 \exp(G_{2i}(t)Z_i)$  according to the following steps:

- (i) Set the initial value of  $t^*$  be 0 for subject  $i$ .
- (ii) Draw a random number  $R \sim \text{Exp}(\bar{\lambda})$ , where  $\bar{\lambda}$  is a fixed value such that  $\lambda_i(t) \leq \bar{\lambda}$ ,  $t$ . Update  $t^* = t^* + R$ .
- (iii) Generate a random number  $V \sim \text{Uniform}(0, 1)$ .
- (iv) Repeat steps (ii) and (iii) until  $V \leq \frac{\lambda_i(t^*)}{\bar{\lambda}}$ , then  $t^*$  become an event time, denoted as  $t_{ij}$  ( $j = 1, 2, \dots$ ).
- (v) If  $t_{ij}$  is within the follow-up time, repeat the process from step (ii) to generate  $t_{i,j+1}$ . If  $t_{ij}$  is larger than the follow-up time, replace  $t_{ij}$  by the follow-up time.

The follow-up period was 12 months from the time of receiving the first dose. Censoring was generated by having 80% of the participants completing the follow-up time and the remaining 20% were uniformly censored between 0.8 and 1.0 of the planned follow-up time. We set  $\lambda_0 = 0.12$  and  $\bar{\lambda} = 0.2$  in the simulation algorithm. Under these settings, for the scenarios with 1000 persons per trial arm, which was similar to the sample size in the case study of malaria chemoprevention, the number of events in the control arm was also similar to that in the case study (about 1500 events). We used 500 replicates per simulation scenario.